

Spatial variability estimation and risk assessment of the aquifer level at sparsely gauged basins using geostatistical methodologies

Emmanouil A. Varouchakis¹ · Kostantinos Kolosionis¹ · George P. Karatzas¹

Received: 23 September 2015 / Accepted: 2 May 2016 / Published online: 6 May 2016
© Springer-Verlag Berlin Heidelberg 2016

Abstract The spatial variability evaluation of the water table level of an aquifer provides useful information in water resources management plans. Three different approaches are applied to estimate the spatial variability of the water table in the study basin. All of them are based on the Kriging methodology. The first is the classical Ordinary Kriging approach, while the second involves information from a secondary variable (surface elevation) and the application of Residual Kriging. The third calculates the probability to lie below a certain groundwater level limit that could cause significant problems in groundwater resources availability. The latter is achieved by means of Indicator Kriging. A recently developed non-linear normalization method is used to transform both data and residuals closer to normal distribution for improved prediction results. In addition, the recently developed Spartan variogram model is applied to determine the spatial dependence of the measurements. The latter proves to be the optimal model, compared to a series of models tested, which provides in combination with the Kriging methodologies the most accurate cross validation estimations. The variogram form is explained with respect to the radius of influence of the pumping wells representing the spatial impact of the pumping activity. Groundwater level and probability maps are developed providing the ability to assess the spatial variability of the groundwater level in the basin and the risk that certain locations have in terms of a safe groundwater level limit that

has been set for the sustainability of the groundwater resources of the basin.

Keywords Geostatistics · Groundwater · Indicator Kriging · Probability maps · Risk assessment · Spartan variogram

Introduction

The knowledge of the spatial variability of the water table level in aquifers with limited monitoring provides information to understand the aquifer behaviour at different locations of the basin. This information becomes more important in basins that are under the threat of over-pumping where the water table has dropped significantly. The spatial distribution feedback gives the potential to identify vulnerable locations. The accurate mapping of groundwater levels in an aquifer is important for effective management and monitoring decisions. However, the number and spatial distribution of hydraulic head measurements are not always sufficient to accurately represent the groundwater level in a given aquifer. Estimates at unsampled locations can be obtained by applying geostatistical methods to the available data in order to map the spatial distribution of an aquifer level. In sparsely monitored basins, accurate mapping of the spatial variability of groundwater level requires the interpolation of scattered data.

Ordinary Kriging (OK) bases its estimates at unsampled locations only on the sampled primary variable. OK interpolation is widely used to determine the spatial variability of groundwater levels in hydrological basins e.g., (Ahmadi and Sedghamiz 2007; Buchanan and Triantafilis 2009; Chung and Rogers 2012; Nikroo et al. 2009; Sun et al. 2009; Theodossiou and Latinopoulos 2006; Varouchakis and Hristopoulos 2013a). Alternatively, Residual Kriging (RK) and Kriging with External Drift (KED), embody secondary information in a

Communicated by: H. A. Babaie

✉ Emmanouil A. Varouchakis
varuhaki@mred.tuc.gr

¹ School of Environmental Engineering, Technical University of Crete, Chania, Greece

drift term. KED and RK are practically equivalent but differ in the methodological steps used (Hengl 2007; Hengl et al. 2003). RK has been applied to the interpolation of water table elevation using deterministic trend models that include e.g. space polynomials (Neuman and Jacobson 1984), topographic metrics such as surface elevation and topographic index, and distance from riverbed (Desbarats et al. 2002; Varouchakis and Hristopoulos 2013b), numerical solutions for the hydraulic head field (Rivest et al. 2008; Varouchakis and Hristopoulos 2013b) and rainfall data (Moukana and Koike 2008).

Indicator Kriging (IK) has been widely used mainly for risk assessment of pollutant concentrations in ground and surface waters leading to significant decision support regarding the prevention and/or remediation of certain sites (Anane et al. 2014; Arslan 2012; Chica-Olmo et al. 2014; Liu et al. 2004; Neshat et al. 2015). However, it can be also applied for the risk assessment of groundwater level spatial distribution in arid areas or in those with high aquifer pumping. Demir et al. (2009) used variable groundwater level thresholds to create indicators under rain and irrigation periods presenting the aquifer response. However, the groundwater level scale was different compared to the scale of this work. In addition, the number of thresholds is important if one aims to assess different scenarios and also to calculate the cumulative effect. This work on the other hand, used a single groundwater level threshold that was calculated from the physical characteristics of the basin, which is under water scarcity threat. The role of this limit is significant as it sets the threshold of balance between pumping and groundwater level necessary for the aquifer sustainability. Other similar works applied Indicator Kriging to address soil saturation probability regarding depth to water table (Lyon et al. 2006a), or to produce probability maps a shallow water table to exceed certain level thresholds per rainfall event (Lyon et al. 2006b). However, most of the works used groundwater level as one of many parameters to perform assessment regarding pollution risk. This work differs from all those, as to the authors knowledge there is not any similar work to address aquifer depletion risk.

The current project presents the application of Ordinary Kriging, Residual Kriging (e.g. surface elevation), and Indicator Kriging to predict the groundwater level spatial variability as well as the associated risk considering an aquifer level threshold respectively in a sparsely gauged basin. In this work the hole-effect property of the Spartan variogram model is presented for the first time in measurement data. The specific shape is obtained when its shape parameter receives negative values. This is an important evidence for the functionality of the Spartan variogram model. Furthermore, the set of a sustainable groundwater level limit based on the physical characteristics of a basin is discussed, risk assessment using IK regarding a groundwater level threshold is interpreted as not many similar works exist and a new dataset is used that has not been published before.

Area of Study

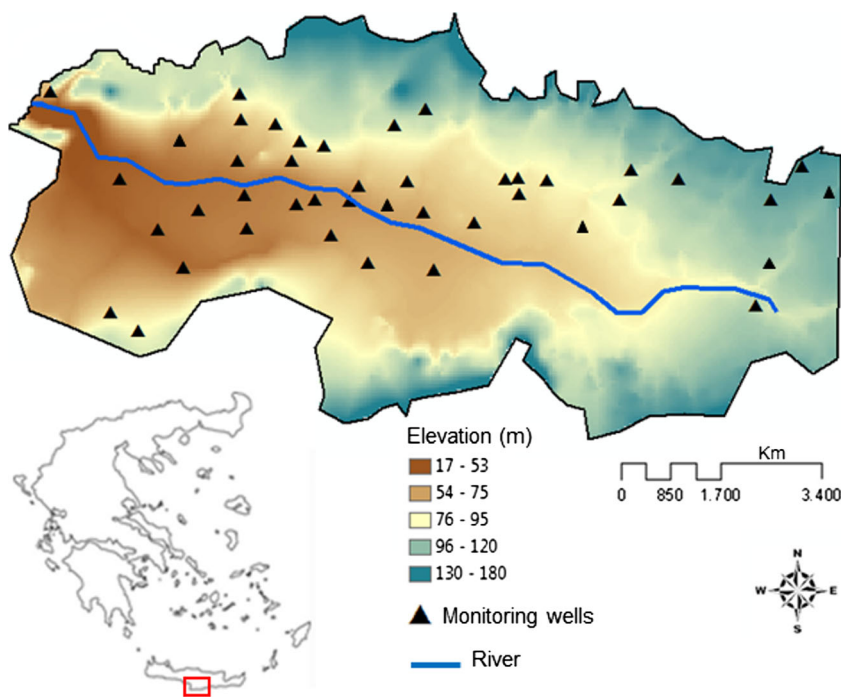
The present research focuses on Mires basin of the Messara Valley (Fig. 1) at the island of Crete (Greece). The study basin consists of an unconfined aquifer, is sparsely sampled and has limited groundwater resources which are vital for the area's ecosystem and agriculture. The mean annual rainfall in Mires basin has been lately estimated around 625 mm. Approximately 65 % of the rainfall is lost to evapotranspiration and 10 % is lost as runoff to the sea, leaving only 25 % to recharge the groundwater store. A detailed hydrogeological and hydrological description of the basin is available in Varouchakis (2016). Knowledge of the spatial variations of the groundwater level is important for developing sound management and monitoring strategies. Over-exploitation during the past 30 years has led to a dramatic decrease, in excess of 35 m, of the groundwater level.

Efficient groundwater management in the basin is crucial in light of predictions based on regional climate change models that show a substantial risk of desertification for Crete. In this work accurate spatial models of the basin's groundwater level are generated that help to identify the susceptible locations and to provide input for potential groundwater resources management plans. The data used in this research consist of hydraulic head measurements (wet period of 2007–2008 hydrological year) from the 43 monitoring locations that operate in the basin which are unevenly distributed and mostly concentrated along a temporary river. The range of hydraulic heads varies from an extremely low value of 11.45 to 72.93 masl. An initial statistical analysis shows that the head data have skewness and kurtosis coefficients equal to $\hat{s}_z = 0.76$ and $\hat{k}_z = 2.80$ respectively, implying a mild deviation from Gaussian statistics ($\hat{s}_z = 0$ and $\hat{k}_z = 3$ respectively). The data analysis is performed by codes developed and run in the Matlab® programming environment (Matlab v.7.10). Standardized spatial coordinates in the interval $[0, 1]$ are used to avoid numerical instabilities.

Methodology

Skewed or erratic data can often be made more suitable for geostatistical modeling by appropriate transformation. A normal distribution for the variable under study is desirable in linear geostatistics (Clark and Harper 2000). Even though normality may not be strictly required, serious violation of normality, such as too high skewness and outliers, can impair the variogram structure and the Kriging results (Gringarten and Deutsch 2001; Ouyang et al. 2006). Ordinary Kriging is well-known to be optimal when the data have a multivariate normal distribution. Transformation of data therefore may be required before Kriging to normalize the data distribution,

Fig. 1 Map of Greece presenting the Messara valley location (red rectangle) in Crete and a topographic map of Mires basin showing the locations of groundwater head measurements along with the corresponding surface elevation and the temporary river path. The black triangles denote the 43 monitoring locations at the basin for the year 2007–08 (modified after Varouchakis and Hristopulos (2013b))



suppress outliers and improve data stationarity (Armstrong 1998; Deutsch and Journel 1992). The estimation then is performed in the Gaussian domain before back-transforming the estimates to the original domain. An advantage of the Gaussian distribution is that spatial variability is easier to be modelled because it reduces effects of extreme values providing more stable variograms (Armstrong 1998; Goovaerts 1997; Pardo-Iguzquiza and Dowd 2005). Kriging represents variability only up to the second order moment (covariance), so the random field of the transformed variable should be Gaussian to derive unbiased estimates at unsampled locations (Deutsch and Journel 1992; Goovaerts et al. 2005).

A non-linear normalizing data transformation is applied in conjunction with Kriging for the accurate prediction of groundwater level spatial variability. The Modified Box-Cox (MBC) transformation method has recently been proposed and applied successfully to normalize hydraulic heads and residuals (Varouchakis et al. 2012). This recently proposed method focuses on normalizing the skewness and kurtosis coefficients of the data, but it neglects higher-order moments (Varouchakis and Hristopulos 2013b). It is defined by the following function,

$$y := g_{MBC}(z; \kappa) = \frac{(z - z_{\min} + k_2^2)^{k_1} - 1}{k_1}, \quad \kappa^T = (k_1, k_2), \tag{1}$$

where k_1 is the power exponent and k_2 is an offset parameter. Use of the latter allows negative z values and so the transformation can be applied to fluctuations as well. Parameters (k_1, k_2) are estimated from the numerical solution of the equations

$\hat{s}_z = 0, \hat{k}_z = 3$ in the form below, where \hat{s}_z and \hat{k}_z are the sample skewness and kurtosis coefficients respectively,

$$\left(\frac{\hat{m}_z - \tilde{m}_z}{\sigma_z} \right)^2 + (\hat{k}_z - 3)^2 \approx 0. \tag{2}$$

In the above equation \hat{m}_z is the sample mean, \tilde{m}_z is the sample’s median and σ_z the standard deviation. The minimization is performed using the Nelder-Mead simplex optimization method (Nelder and Mead 1965; Press et al. 1992).

Besides the classical OK interpolation, the prediction of the hydraulic head spatial variability is also performed using RK by incorporating local geographic features, such as the ground surface elevation in the trend function. Previous studies have shown that incorporating such auxiliary information in the trend function improves the accuracy of the spatial interpolation (Varouchakis 2012). Herein, there are two reasons for employing ground surface elevation as an auxiliary variable. The first is the important correlation between surface elevation and groundwater level; at high elevation the groundwater level is also high following a decreasing trend towards lower elevations. The second reason is the application of a tool by Haitjema and Mitchell-Braker (2005). This tool examines if the aquifer is recharge or topography controlled. The equation that describes the tool involves the average annual recharge rate R [m/d], the average distance between surface waters, L [m], a factor m between 8 and 16 for aquifers that are strip like or circular in shape respectively, the (horizontal) aquifer hydraulic conductivity, k [m/d], the aquifer thickness, H [m] and

the maximum distance between the average surface water levels and the terrain elevation, d [m].

$$\frac{RL^2}{mkHd} \begin{cases} > 1, & \text{topography controlled} \\ < 1, & \text{recharge controlled} \end{cases} \quad (3)$$

Although Mires aquifer does not comply exactly with the conditions applied to produce this inequality, an estimate can be obtained. The surface waters in the basin are limited and there is only a main river crossing the plain. Therefore, a distance between surface waters cannot be exactly defined. However, the eastern and western parts of the main river are connected with two tributaries that their in between distance can define the variable L (approximately 15,000 m). On the other hand, the aquifer is partly circular in shape at the up-stream and stripe like at the down-stream. Thus m on average would be set equal to 12. The other variables are based on average aquifer values: $k = 50$ m/d, $R = 0.0004$ m/d, $H = 21.5$ m and $d = 10$ m (Varouchakis 2015). Solving Eq. (3) the calculated ratio is equal to 0.7 and thus less than 1. This result means that the aquifer is recharge controlled. However, the result is quite close to 1 and one can assume that topography has also a vital role. Thus, considering also the important relation between the elevation and the groundwater level trend (65 %) and based on the absence of information on the spatial distribution of recharge in the basin, one can use the ground surface elevation as an auxiliary variable. Its significance and usefulness will be assessed based on the derived results.

In the following, it is assumed that the water table level is represented by a spatial random field (SRF), $Z(\mathbf{s} \in S)$, where S is the set of sampling points with cardinal number N . The values of the SRF in a given state will be denoted by lower-case letters. The target is to derive estimates, $\hat{Z}(\mathbf{s} \in P)$ of the water table elevation at the prediction set points, P that lie on a rectangular grid that covers the basin. Therefore, \mathbf{s}_i , $i = 1, \dots, N$ denote the sampling points, $z(\mathbf{s}_i)$ are the head values (in masl) at these points, and \mathbf{s}_0 denotes an estimation point, which is assumed to lie inside the convex hull of the sampling network. For mapping purposes, it is assumed that \mathbf{s}_0 moves sequentially through all the nodes of the mapping grid.

Spatial interpolation of the groundwater levels was initially applied by means of OK and RK in combination with MBC normalizing transformation, while IK based on developed indicators from the data was then implemented. In the first approach, a normalizing transformation $g(\cdot)$ is applied to the data. Then, OK is used to predict the transformed field $Y(\mathbf{s}) = g(Z(\mathbf{s}))$, and the predictions are back-transformed to obtain head estimates. In the second approach, a trend model $m_Z(\mathbf{s})$ is introduced that captures local features. Since the fluctuation SRF, $Z'(\mathbf{s}) = Z(\mathbf{s}) - m_Z(\mathbf{s})$, is non-Gaussian, a transformation $g(\cdot)$ is applied to obtain a normalized SRF, $Y(\mathbf{s}) = g(Z'(\mathbf{s}))$. The experimental variogram is then estimated and is fitted to theoretical models. Next, the Gaussian field

$\hat{Y}(\mathbf{s} \in P)$ is estimated at the prediction points using OK. Finally, head estimates are retrieved from $\hat{Y}(\mathbf{s} \in P)$ by applying the back-transformation and adding the trend. Leave-one-out cross-validation analysis was used to determine the optimal spatial model applied to water table level data and to assess the accuracy of the interpolated head field.

Spatial dependence

The variogram is commonly used in geostatistical analysis to measure the spatial dependence between neighboring observations. The omnidirectional empirical (experimental) variogram of the hydraulic head and of the residuals was determined using the method of moments. The empirical variogram was fitted with isotropic classical models (Gaussian, Exponential, Linear, Spherical, and Power-law), the Matérn model (Goovaerts 1997), and the new family of Spartan variograms (3D, 2D models) (Hristopulos 2003; Hristopulos and Elogne 2007).

Spartan Spatial Random Fields (SSRFs) are a geostatistical model (Hristopulos 2002, 2003) inspired from statistical field theory with applications in environmental risk assessment and environmental monitoring (Elogne et al. 2008; Elogne and Hristopulos 2008; Hristopulos and Elogne 2009). SSRFs are generalized Gibbs random fields with an energy functional that is based on local interactions between the field values. The term Spartan indicates parametrically compact model families that involve a small number of parameters. SSRFs provide a new class of generalized covariance functions. The SSRFs covariance functions can be used for spatial interpolation with the classical Kriging estimators. Spartan covariance and variogram functions have been applied to various environmental data sets (Elogne et al. 2008; Varouchakis and Hristopulos 2013b). Herein, the Spartan covariance derived for $d = 3$ dimensions is applied.

The model parameters are obtained by fitting the SSRFs function (4) to the experimental variogram (Hristopulos and Elogne 2007). The exponential covariance is formed for $\eta_1 = 2$, while for $|\eta_1| < 2$ the product of the exponential and hole-effect model is obtained. According to Christakos (1991) a covariance function that is permissible in three spatial dimensions is also permissible in two dimensions. The components of the equation are presented and explained in Table 1.

$$C_z(\mathbf{h}) = \begin{cases} \frac{\eta_0 e^{-h\beta_2}}{2\pi\sqrt{|\eta_1^2-4|}} \left[\frac{\sin(h\beta_1)}{h\beta_1} \right], & \text{for } |\eta_1| < 2, \quad \sigma_z^2 = \frac{\eta_0}{2\pi\sqrt{|\eta_1^2-4|}} \\ \frac{\eta_0 e^{-h}}{8\pi}, & \text{for } \eta_1 = 2, \quad \sigma_z^2 = \frac{\eta_0}{8\pi} \\ \frac{\eta_0 (e^{-h\omega_1} - e^{-h\omega_2})}{4\pi(\omega_2 - \omega_1)h\sqrt{|\eta_1^2-4|}}, & \text{for } \eta_1 > 2, \quad \sigma_z^2 = \frac{\eta_0}{4\pi\sqrt{|\eta_1^2-4|}} \end{cases} \quad (4)$$

Table 1 Interpretation of the Spartan covariance function components

Spartan function components	Interpretation
η_0	Scale factor
η_1	Rigidity coefficient
$\beta_1 = 2 - \eta_1 ^{1/2}/2$	Dimensionless wavenumber
$\beta_2 = 2 + \eta_1 ^{1/2}/2$ and $\omega_{1,2} = (\eta_1 \mp \Delta /2)^{1/2}$, $\Delta = \eta_1^2 - 4 ^{1/2}$,	Dimensionless damping coefficients
ξ	Characteristic length
$\mathbf{h} = \mathbf{r}/\xi$	Normalized lag vector
$h = \mathbf{h} $	Its Euclidean norm
σ_z^2	Variance

Spatial models

In spatial linear interpolation methods such as OK and RK, it generally holds that,

$$\hat{z}(\mathbf{s}_0) = \sum_{\{i:\mathbf{s}_i \in \mathbb{S}_0\}} \lambda_i z(\mathbf{s}_i), \tag{5}$$

where \mathbb{S}_0 is the set of sampling points in the search neighborhood of \mathbf{s}_0 . The neighborhood is empirically chosen so as to optimize the cross validation measures. The weights λ_i are obtained by minimizing the mean square estimation error conditionally on the zero-bias constraint (Cressie 1993) and they depend on the variogram model $\gamma_z(\mathbf{r})$, where \mathbf{r} are the spatial lags of the experimental variogram (Deutsch and Journel 1992). The OK estimation variance is given by the following equation, with the Lagrange coefficient μ compensating for the uncertainty of the mean value:

$$\sigma_E^2(\mathbf{s}_0) = \sum_{\{i:\mathbf{s}_i \in \mathbb{S}_0\}} \lambda_i \gamma_z(\mathbf{s}_i, \mathbf{s}_0) + \mu. \tag{6}$$

Overall OK variance is termed as the weighted average of variograms from the new point \mathbf{s}_0 to all calibration points \mathbf{s}_j , plus the Lagrange multiplier.

RK combines a trend function with interpolation of the residuals. Herein, a deterministic trend is applied based on the basin topography. In RK the estimate is expressed as:

$$\hat{z}(\mathbf{s}_0) = m_z(\mathbf{s}_0) + \hat{z}'(\mathbf{s}_0), \tag{7}$$

where $m_z(\mathbf{s}_0)$ is the trend function, and $\hat{z}'(\mathbf{s}_0)$ is the interpolated residual by means of OK (Rivoirard 2002). Typically, the trend function is modeled as:

$$m_z(\mathbf{s}_0) = \sum_{k=0}^p \beta_k q_k(\mathbf{s}_0); \quad q_k(\mathbf{s}_0) \equiv 1, \tag{8}$$

where $q_k(\mathbf{s}_0)$ are the values of auxiliary variables at \mathbf{s}_0 , β_k are the estimated regression coefficients and p is the number of auxiliary variables (Draper and Smith 1981; Hengl 2007;

Hengl et al. 2007). The regression coefficients are estimated from the sample using ordinary least squares (OLS) (Kitanidis 1993). The variance of the estimates follows from the equation (Hengl 2007; Hengl et al. 2003):

$$\sigma^2(\mathbf{s}_0) = \sigma_d^2(\mathbf{s}_0) + \sigma_f^2(\mathbf{s}_0), \tag{9}$$

$$\sigma_d^2(\mathbf{s}_0) = \mathbf{q}_0^T (\mathbf{q}^T \gamma_z^{-1} \mathbf{q})^{-1} \mathbf{q}_0, \tag{10}$$

$$\sigma_f^2(\mathbf{s}_0) = \sum_{\{i:\mathbf{s}_i \in \mathbb{S}_0\}} \lambda_i \gamma_z'(\mathbf{s}_i, \mathbf{s}_0) + \mu, \tag{11}$$

where $\sigma_d^2(\mathbf{s}_0)$ is the drift prediction variance, \mathbf{q}_0 is the vector of $(p + 1) \times 1$ predictors at the unvisited location, \mathbf{q} is the matrix of $(N_0 + 1) \times (p + 1)$ predictors at the sampling points in the search neighborhood (N_0 is the number of points within the search neighborhood of \mathbf{s}_0), γ_z' is the variogram matrix of the $(N_0 + 1) \times (N_0 + 1)$ residuals at the measured locations (neighborhood) and $\sigma_f^2(\mathbf{s}_0)$ is the kriging (OK) variance of residuals.

Herein a trend model for Mires basin groundwater level data is presented. Following other studies, based on the fact that usually the water table level of an unconfined aquifer follows the elevation trend, secondary information in the trend is considered from a Digital Elevation Model (DEM) of the area (Desbarats et al. 2002; Deutsch and Journel 1992; Goovaerts 1997; Hoeksema et al. 1989; Nikroo et al. 2009; Rivest et al. 2008). This choice was supported by the interpretation provided earlier in the Methodology section, and primarily by the important correlation coefficient between the groundwater level and the ground surface elevation in the basin ($R=0.65$, is characterized as important correlation (Tichy 1993)). A scatter plot of ground surface elevation vs groundwater level is presented in Fig. 2.

The following expression for the trend of the hydraulic head (in masl) is applied (T-DEM):

$$m_z(\mathbf{s}) = f \text{ DEM}(\mathbf{s}) + c, \tag{12}$$

where f, c are linear coefficients and $DEM(\mathbf{s})$ is the local DEM value.

Another interpolation method applied is IK. This is a non-parametric geostatistical method for estimating the probability of a variable to exceed or lie below a specific threshold value at a given location (Goovaerts 1997). In this work, IK is applied for mapping the risk associated with a specified groundwater level limit that could lead to significant problem of groundwater availability. A critical aquifer level limit for the basin’s groundwater resources availability can be set in terms of a statistical and a physical based approach. The first involves the 25th, lower, percentile of the available data values which is equal to 25 m above sea level (m.a.s.l). This value was validated by a physically based approach that involves physical characteristics of the basin. The aquifer capacity has been recently estimated equal to 55 Mm³, the aquifer area equal to 26.1 km² and the porosity equal to 0.085. Dividing the first two figures and then their result with the porosity the aquifer level is calculated. This is equal to 24.7 m.a.s.l, similar to the lower percentile of the available data. Thus, 25 m.a.s.l can be set as the aquifer level threshold for sustainable groundwater resources management at the basin.

IK is applied to determine the conditional probability at unsampled points based on the spatial dependence structure of indicator-transformed data points with a binary distribution (e.g. 0 and 1). IK proceeds as the classical Ordinary Kriging (the main change is the choice of a cutoff value) with the difference that results is now maps with values between 0 and 1 expressing probability a condition to apply (Chica-Olmo et al. 2014; Deutsch and Journel 1992). Indicator variogram analysis is also performed using the models and the procedure previously stated for OK and RK (Isaaks and Srivastava 1989).

This method does not make assumptions regarding the variables distribution and has the ability to take into account, to a large extent, the uncertainty of the data. The IK is based on the conversion of all data from continuous to a binary form

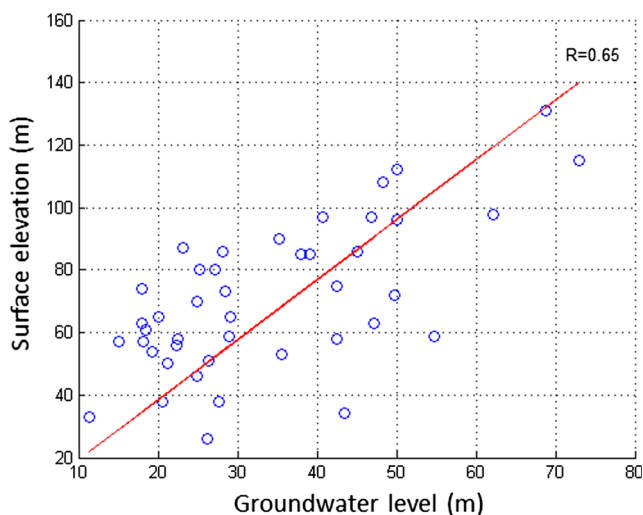


Fig. 2 Scatter plot of groundwater level (m) vs surface elevation (m)

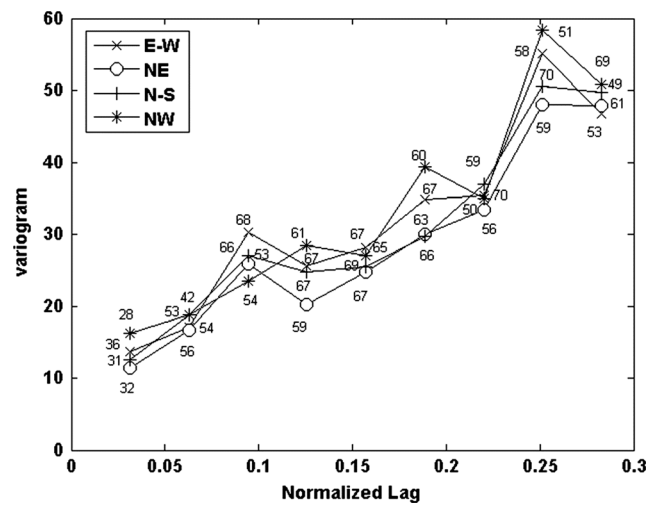


Fig. 3 Experimental directional variograms of groundwater level fluctuations with 30° angle tolerance along the four main geographical directions, E–W, N–S, NE and NW

according to a specific threshold value. Thus, is robust to outliers handling. This value can be either a percentile of our data or a default value of marginal importance for the system under study. Subsequently, data with values below the threshold take a value of 1, while the remaining taking a value of 0.

$$I(z(\mathbf{s})) = \begin{cases} 1, & z(\mathbf{s}) \leq z' \\ 0, & \text{otherwise} \end{cases} \quad (13)$$

where, $I(z(\mathbf{s}))$ is a binary variable, $z(\mathbf{s})$ is the measured value and z' is the cut-off (threshold) value.

Indicator Kriging is a geostatistical method best suited for issues that involve a threshold value (Goovaerts 1999; Isaaks and Srivastava 1989; Webster and Oliver 2001). However, most practical problems that require indicator techniques require well-chosen threshold which have a special significance to the problem being addressed. Probability maps delineate suitable and unsuitable sites regarding the examined issue, while help to take decisions to prevent and/or remediate a site compared to locations with reduced or no risk.

The method proceeds as follows: a) convert the given values to indicators: divide the range evenly or based on different quintiles ($q_{0.25}$; $q_{0.50}$; $q_{0.75}$), b) estimate the indicator variogram, c) apply Kriging using the usual equations and obtain predictions. On the other hand, the methodology has a set of disadvantages such as it will not necessarily provide

Table 2 Normalization results using Modified Box-Cox (MBC) transformation: skewness coefficient \hat{s}_z ; kurtosis coefficient \hat{k}_z

	\hat{s}_z	\hat{k}_z
Initial head data	0.76	2.80
MBC	-0.15	2.99

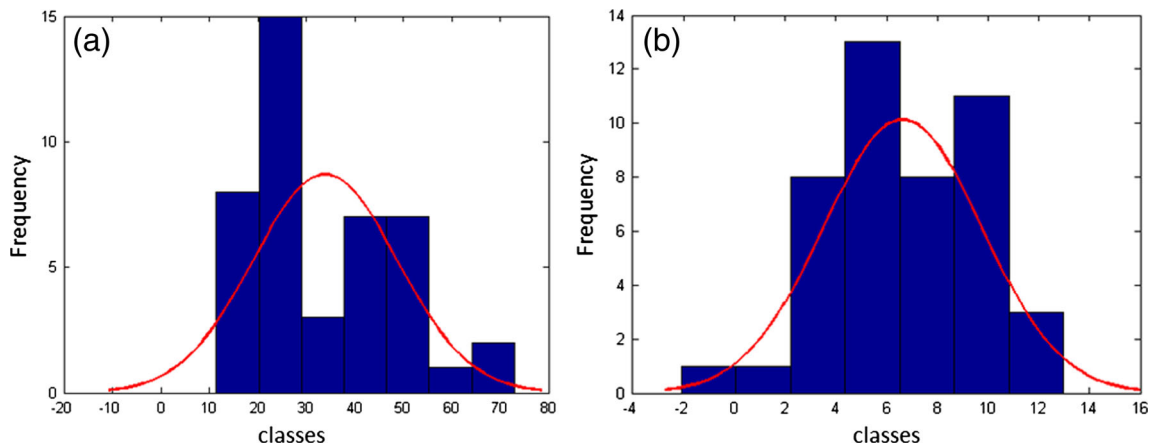


Fig. 4 Histograms of the groundwater level data before (a) and after (b) the transformation with MBC

probabilities to add up to 1 and sometimes the prediction may end up beyond the zero to one interval, e.g. Kriging occasionally provides negative weights-screening effect (Goovaerts 1997; Papadopoulou et al. 2009).

Results and Discussion

The performance of the Kriging-based geostatistical models is evaluated by using the leave one out cross validation technique that is usually applied in small datasets (Witten et al. 2011). A series of well-known statistical measures is employed to compare the true and estimated values of the cross-validation procedure, such as the correlation coefficient *R*, the Mean Absolute Error (MAE), the Root Mean Square Error (RMSE) and the Mean Absolute Relative Error (MARE).

Anisotropy was investigated by comparing directional variograms in four main directions (Goovaerts 1997) using an angle tolerance of 30°. Smaller tolerance values (15°) do not permit a sufficient number of data pairs (i.e., at least 30) at each lag. According to Journel and Huijbregts (1978), in order to acquire a good variogram, there should be approximately 30 pairs of distances and values for every lag. In addition the number of lags was reduced in order to achieve the required pair number for directional variograms. As shown in Fig. 3, there is no clear difference among the directional variograms

for the original data. In addition a test of geometric anisotropy was performed based on the method of Covariance Hessian Identity (Chorti and Hristopulos 2008; Hristopulos 2002). This method is non-parametric, in the sense that it provides an estimate of the aspect ratio (i.e. the ratio of the two principal correlation lengths) and the orientation of the principal axes, without requiring variogram estimation and modeling. The aspect ratio is thus estimated at 0.75, while the short principal axis is rotated by 8° with respect to the E-W direction. The value of 0.75 does not differ significantly from unity. Indeed, the isotropic hypothesis cannot be rejected with 95 % confidence for ratios in the range [0.70 – 1.07] using the test given (Spiliopoulos et al. 2011). In light of the above analysis, the variogram function of the groundwater level is considered to be isotropic (Ahmadi and Sedghamiz 2007).

The general approach that is used for interpolation applies a normalizing transformation followed by OK on the transformed variables, and it finally back-transforms the predictions. The application of MBC methodology to the initial head dataset improves their normality (Table 2). The normality improvement is also supported by histograms of the data before and after the transformation (Fig. 4).

In terms of the spatial model that considers the head data the parameters of the theoretical variogram models tested are obtained by least squares fitting to the experimental omnidirectional variogram of the transformed hydraulic head. The 3D Spartan model gives the best fit in terms of cross validation

Table 3 Cross validation measures for spatial MBC-OK model with optimal variograms: MBC & OK: Ordinary Kriging with modified Box-Cox transformation of data and back-transformation

Variogram model	MAE (masl)	BIAS (masl)	MARE	RMSE (masl)	<i>R</i>
SP	5.32	0.03	0.17	7.20	0.90
SPH	5.41	0.08	0.17	7.43	0.90
M	5.65	0.04	0.18	7.70	0.89

SP Spartan variogram, *SPH* Spherical variogram, *M* Matérn variogram

Table 4 Skewness \hat{s}_z and kurtosis \hat{k}_z coefficients of trend models residuals following modified Box-Cox (MBC) normalization

	\hat{s}_z	\hat{k}_z
Residuals	0.35	2.5
MBC	-0.10	3.0

results (Table 3) while the Spherical and the Matérn variogram come close. The 2D Spartan function did not provide a good fit for this dataset.

In the case of spatial model with trend component, RK is applied. RK combines a trend function with interpolation of the residuals. The residuals of the trend model also display deviations from normality that are reduced by means of the MBC transformation (Table 4). Similarly, histograms (Fig. 5) present the normality improvement.

The omnidirectional experimental variogram is calculated by applying the method of moments to the transformed residuals of the T-DEM model. The Spartan variogram model (Fig. 6) again provides the best fit in terms of cross validation results (Table 5). The Spherical variogram provides similar results to the Spartan model while third best is the Matérn model.

Another method to test data normality improvement, is the non-parametric Kolmogorov-Smirnov test. The test is applied to examine if a sample comes from a reference probability Distribution (Massey 1951). The test was implemented in Matlab® environment using the function «kstest» for both the transformed datasets. The null hypothesis for the Kolmogorov-Smirnov test is that data follows the standard normal distribution. Therefore, the null hypothesis was not rejected for the transformed datasets at significant levels 5 % and of 10 %.

The MBC-RK approach improves significantly the mean absolute prediction error (4.27 masl) by over 1 m compared to

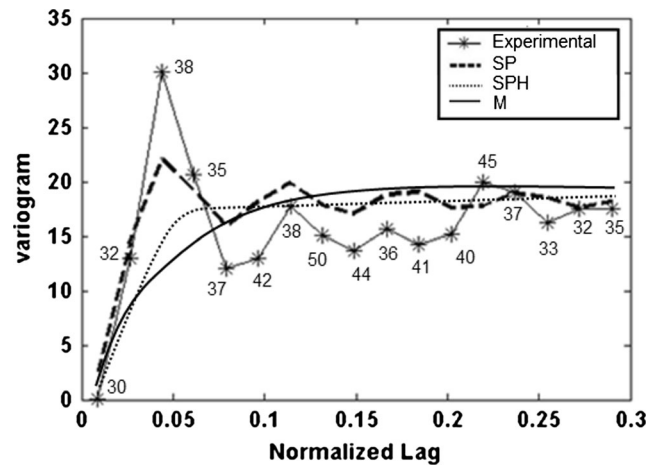


Fig. 6 Plot of omnidirectional variogram of residuals (*stars*) after applying MBC normalization and the best-fitted variogram models. The residuals are derived by applying to the trend the ground surface elevation (T-DEM). The number of pairs used at each lag distance (17 lags) are also shown on the plot

the MBC-OK (5.32 masl) approach. In addition the other estimation measures are at least similar (BIAS) but mostly improved (RMSE, R, MARE). Considering overall the cross validation measures the estimates based on the Spartan model prevails compared to the other two optimal models.

The least squares sum for each fitted variogram model is considered, which is an index of optimal fitting, for selecting the optimal variogram model with Indicator Kriging interpolation. Spartan model achieves the best fit (Fig. 7) over the range of lags considered providing a value of 0.023 compared to 0.029 for the spherical and 0.031 for the Matérn models.

The T-DEM trend model with RK and the IK methodology are applied to estimate the groundwater level and the probabilities of groundwater level to lie below a threshold value on a 100 × 100 grid defined in normalized coordinate space (actual cell size: 114 × 47 m). In addition the uncertainties of the estimations are also determined on a same grid size. Estimates are obtained only at points that lie inside the convex hull of the

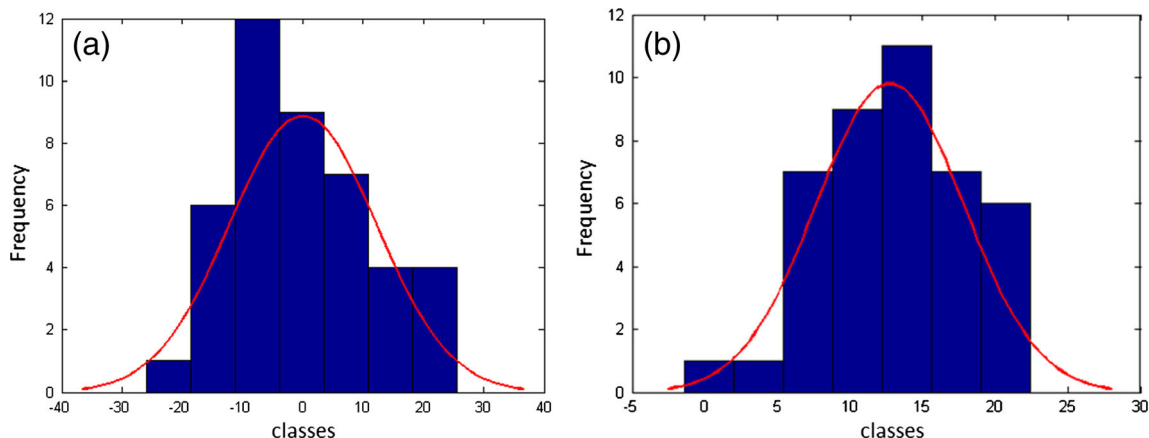


Fig. 5 Histograms of the trend model residuals before (a) and after (b) the transformation with MBC

Table 5 Cross validation measures for spatial MBC-RK-T-DEM model with optimal variograms: T-DEM trend using DEM surface elevation

Variogram model	MAE (masl)	BIAS (masl)	MARE	RMSE (masl)	R
SP	4.27	0.07	0.15	5.90	0.91
SPH	4.46	0.05	0.15	6.23	0.90
M	4.75	0.08	0.16	6.50	0.88

MBC & RK: Residual Kriging with modified Box-Cox transformation of residuals and back-transformation
 SP Spartan variogram, SPH Spherical variogram, M Matérn variogram

measurement locations (7317 grid points). The contour maps in physical space are shown in Figs. 8, 9, 10, and 11. The residuals of the T-DEM model are interpolated using the Spartan variogram model (Fig. 6) with the following optimal parameter values: $\sigma^2 = 17.77$, $\xi = 0.27$ (in normalized units), $\eta_1 = -1.99$ while the indicators applying the Spartan variogram model (Fig. 7) with optimal parameter values: $\sigma^2 = 0.25$, $\xi = 0.26$ (in normalized units), $\eta_1 = -1.90$. The optimum search radius used with the Spartan model (determined by the leave-one-out cross validation test) is equal to 0.38 (normalized units) for both models. Near the origin and at intermediate distances, which are crucial for the interpolation, the Spartan model fitting is very good and overall follows closely the trend of the experimental variogram. The negative values of η_1 causes a negative hole effect in the Spartan correlation (Žukovič and Hristopulos 2008) that can be observed in both variogram figures (Figs. 6 and 7).

The groundwater level map of the basin (Fig. 8) presents the spatial variability of the groundwater level that change from East towards West direction following the ground surface elevation trend (Fig. 1). The higher levels are met at the East of the basin while the lowest towards the West. The error map (Fig. 9) identifies the locations of the Mires Basin with the largest Kriging standard deviation. Hence, the borders of the basin can benefit from further sampling according to RK standard deviation results.

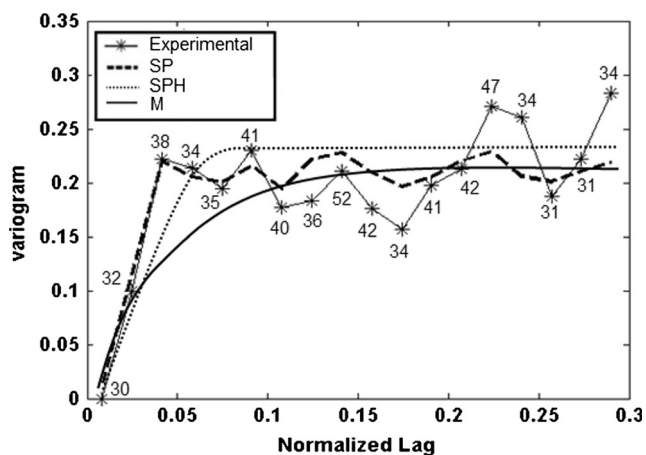


Fig. 7 Indicator omnidirectional variogram and the best-fitted variogram models. The number of pairs used at each lag distance (18 lags) are also shown on the plot

Indicator Kriging predictions (Fig. 10) shows that in the center and towards the West borders of the basin the risk of the aquifer level to decline below the set 25 m.a.s.l threshold is significant. Probabilities are increased closer to the river path than higher away. The dependence is reasonable considering that the agricultural activity in the area is concentrated along the temporary river.

Estimation variance calculated through IK is usually highest where wells distribution density is poor and variability among neighbouring observations is large, while lowest where wells distribution is good and variability is low (Hohn 1999). The variance range though depends on the quality of the fitted theoretical variogram model. The accurate knowledge of the correlation between point measurements at different locations produces estimates of the prediction variance that are minimal. This is succeeded when the fit of the model variogram to the experimental is the optimum, as occurs herein (Fig. 7). Thus, the properties of the variogram model occur through the whole area of interest leading to accurate estimates with low variance even for regions of poor monitoring density.

Significantly low IK variance values (maximum variance is equal to 0.0525) are obtained herein due to the optimum spatial dependence inference that is provided by Spartan variogram model (Fig. 7). According to Chiles and Delfiner (1999) the computed kriging variance is directly affected by the variogram fit. In this work IK variance (Fig. 11) is very low even at ungauged locations of 0 or close to 1 probability

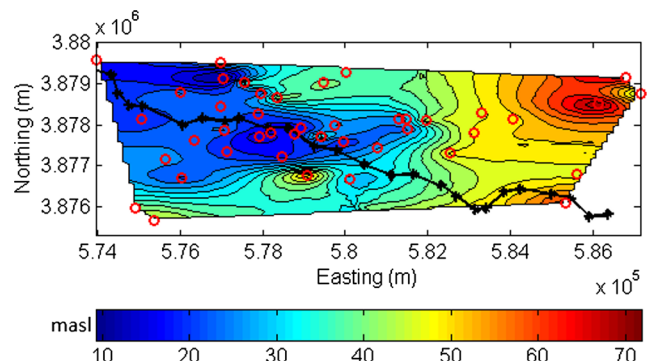


Fig. 8 Map of estimated groundwater level in the Mires basin using MBC-RK-T-DEM spatial model, adapted on the real basin coordinates and location in the valley (circles denote the monitoring locations and solid black line the temporary river path)

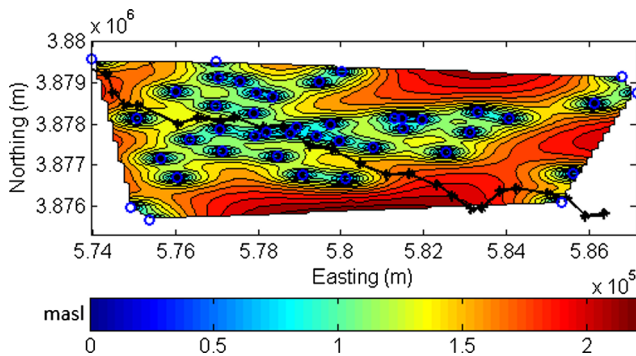


Fig. 9 Map of estimated groundwater level standard deviation in the Mires basin using MBC-RK-T-DEM spatial model, adapted on the real basin coordinates and location in the valley (circles denote the monitoring locations and solid black line the temporary river path)

the groundwater level to lie below the set threshold value. Therefore, no further variance analysis is required such as conditional simulations to calculate the cumulative distribution function of the predictions (Deutsch and Journel 1992; Goovaerts 1997; Kanevski et al. 2009; Olea 1999).

The final risk (probability) map (Fig. 10), considering the calculated variance of the estimates (Fig. 11), shows that around 25 % of the aquifer's surface present significant probability the aquifer level to lie below the 25 m.a.s.l. This area corresponds to almost 40 % of the productive agricultural land of the basin.

A very interesting characteristic that is identified in this work is the shape of the modeled Spartan variogram. According to a previous work (Varouchakis and Hristopulos 2013b) this shape can be explained with respect to the pumping activity of the basin. The average distance between the increment and the decrement in the variograms is equal to 150 m that lies between the range 105 to 160 m, which correspond to the radii of influence range of the pumping wells in Mires basin (Varouchakis and Hristopulos 2013b). Therefore, the trend of the experimental and of the model variogram expresses the aquifer behavior under pumping activity. As it

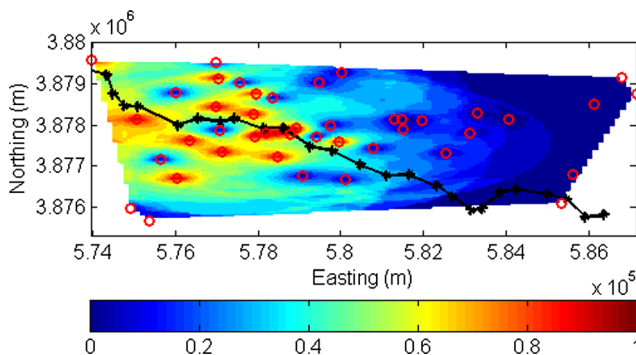


Fig. 10 Map of estimated probabilities the aquifer level to decline below the set 25 m.a.s.l. threshold value in Mires basin using IK, adapted on the real basin coordinates and location in the valley (circles denote the monitoring locations and solid black line the temporary river path)

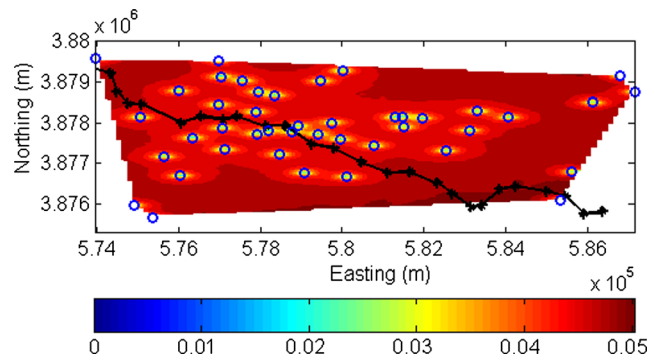


Fig. 11 Map of estimated probabilities variance in the Mires basin using IK, adapted on the real basin coordinates and location in the valley (circles denote the monitoring locations and solid black line the temporary river path)

has been stated in a previous work more than 200 wells operate in the basin affecting the measurements at the monitoring locations (Varouchakis and Hristopulos 2013b).

Conclusions

The optimal spatial interpolation approach for the spatial variability of the groundwater level in Mires basin is based on Residual Kriging with the Spartan variogram model applied to the normalized (MBC) fluctuations. The present findings are supported by the results of cross validation analysis. In addition, risk maps based on IK identify the vulnerable areas of the basin that require intense monitoring and remedial actions to avoid further decline of the aquifer. These are located at the west part of the basin mainly along the river path. The recently developed MBC transformation method shows an excellent behaviour transforming both data and residuals closer to normal distribution. In addition the Spartan variogram model has an excellent fit to the experimental variogram of the data, residuals and indicators following closely their trend. Thus, it constitutes a reliable alternative to assess the spatial dependence of groundwater level data in interpolation studies.

References

- Ahmadi S, Sedghamiz A (2007) Geostatistical analysis of spatial and temporal variations of groundwater level. *Environ Monit Assess* 129(1):277–294
- Anane M, Selmi Y, Limam A, Jedidi N, Jellali S (2014) Does irrigation with reclaimed water significantly pollute shallow aquifer with nitrate and salinity? An assay in a perurban area in North Tunisia. *Environ Monit Assess* 186(7):4367–4390
- Armstrong M (1998) *Basic linear geostatistics*. Springer Verlag, Berlin
- Arslan H (2012) Spatial and temporal mapping of groundwater salinity using ordinary kriging and indicator kriging: the case of Bafra Plain, Turkey. *Agric Water Manag* 113:57–63

- Buchanan S, Triantafyllis J (2009) Mapping water table depth using geophysical and environmental variables. *Ground Water* 47(1):80–96
- Chica-Olmo M, Luque-Espinar JA, Rodriguez-Galiano V, Pardo-Igúzquiza E, Chica-Rivas L (2014) Categorical Indicator Kriging for assessing the risk of groundwater nitrate pollution: the case of Vega de Granada aquifer (SE Spain). *Sci Total Environ* 470–471:229–239
- Chiles JP, Delfiner A (1999) *Geostatistics (modeling spatial uncertainty)*. Wiley, New York
- Chorti A, Hristopulos DT (2008) Non-parametric identification of anisotropic (elliptic) correlations in spatially distributed data sets. *IEEE Trans Signal Process* 56(10):4738–4751
- Christakos G (1991) *Random field models in earth sciences*. Academic, San Diego
- Chung J-W, Rogers JD (2012) Interpolations of groundwater table elevation in dissected uplands. *Ground Water* 50(4):598–607
- Clark I, Harper WV (2000) *Practical geostatistics 2000*. Ecosse North America Llc., Columbus
- Cressie N (1993) *Statistics for spatial data (revised ed.)*. Wiley, New York
- Demir Y, Erşahin S, Güler M, Cemek B, Günel H, Arslan H (2009) Spatial variability of depth and salinity of groundwater under irrigated ustifluents in the Middle Black Sea Region of Turkey. *Environ Monit Assess* 158(1–4):279–294
- Desbarats AJ, Logan CE, Hinton MJ, Sharpe DR (2002) On the kriging of water table elevations using collateral information from a digital elevation model. *J Hydrol* 255(1–4):25–38
- Deutsch CV, Journel AG (1992) *GSLIB. Geostatistical software library and user's guide*. Oxford University Press, New York
- Draper N, Smith H (1981) *Applied regression analysis*, 2nd edn. Wiley, New York
- Elogne SN, Hristopulos DT (2008) Geostatistical applications of Spartan spatial random fields. In: Soares A, Pereira MJ, Dimitrakopoulos R (eds) *geoENV VI—geostatistics for environmental applications in series: quantitative geology and geostatistics*, vol 15. Springer, Berlin, pp 477–488
- Elogne S, Hristopulos D, Varouchakis E (2008) An application of Spartan spatial random fields in environmental mapping: focus on automatic mapping capabilities. *Stoch Env Res Risk A* 22(5):633–646
- Goovaerts P (1997) *Geostatistics for natural resources evaluation*. Oxford University Press, New York
- Goovaerts P (1999) Geostatistics in soil science: state-of-the-art and perspectives. *Geoderma* 89(1–2):1–45
- Goovaerts P, AvRuskin G, Meliker J, Slotnick M, Jacquez G, Nriagu J (2005) Geostatistical modeling of the spatial variability of arsenic in groundwater of southeast Michigan. *Water Resour Res* 41, W07013. doi:10.1029/2004WR003705
- Gringarten E, Deutsch CV (2001) Teacher's aide: variogram interpretation and modeling. *Math Geol* 33(2001):507–534
- Haitjema HM, Mitchell-Bruker S (2005) Are water tables a subdued replica of the topography? *Ground Water* 43(6):781–786
- Hengl T (2007) *A practical guide to geostatistical mapping of environmental variables*. Office for Official Publications of the European Communities EUR 22904 EN-Scientific and Technical Research series 143
- Hengl T, Heuvelink GBM, Stein A (2003) Comparison of kriging with external drift and regression-kriging. International Institute for Geoinformation Science and Earth Observation (ITC) Technical note 17
- Hengl T, Heuvelink GBM, Rossiter DG (2007) About regression-kriging: from equations to case studies. *Comput Geosci* 33(10):1301–1315
- Hoeksema RJ, Clapp RB, Thomas AL, Hunley AE, Farrow ND, Dearstone KC (1989) Cokriging model for estimation of water table elevation. *Water Resour Res* 25(3):429–438
- Hohn ME (1999) *Geostatistics and petroleum geology*. Springer, Dordrecht
- Hristopulos DT (2002) New anisotropic covariance models and estimation of anisotropic parameters based on the covariance tensor identity. *Stoch Env Res Risk A* 16(1):43–62
- Hristopulos DT (2003) Spartan Gibbs random field models for geostatistical applications. *SIAM J Sci Comput* 24(6):2125–2162
- Hristopulos DT, Elogne SN (2007) Analytic properties and covariance functions for a new class of generalized Gibbs random fields. *IEEE Trans Inform Theory* 53(12):4667–4679
- Hristopulos DT, Elogne SN (2009) Computationally efficient spatial interpolators based on Spartan spatial random fields. *IEEE Trans Signal Process* 57(9):3475–3487
- Isaaks EH, Srivastava RM (1989) *An introduction to applied geostatistics*. Oxford University Press, New York
- Journel AG, Huijbregts C (1978) *Mining geostatistics*. Academic, New York
- Kanevski M, Pozdnoukhov A, Timonin V (2009) *Machine learning for spatial environmental data: theory, applications, and software*. EPFL press, Lausanne
- Kitanidis P (1993) Generalized covariance functions in estimation. *Math Geol* 25(5):525–540
- Liu C-W, Jang C-S, Liao C-M (2004) Evaluation of arsenic contamination potential using indicator kriging in the Yun-Lin aquifer (Taiwan). *Sci Total Environ* 321(1–3):173–188
- Lyon SW, Lembo AJ Jr, Walter MT, Steenhuis TS (2006a) Defining probability of saturation with indicator kriging on hard and soft data. *Adv Water Resour* 29(2):181–193
- Lyon SW, Seibert J, Lembo AJ, Walter MT, Steenhuis TS (2006b) Geostatistical investigation into the temporal evolution of spatial structure in a shallow water table. *Hydrol Earth Syst Sci* 10(1):113–125
- Massey FJ (1951) The Kolmogorov-Smirnov test for goodness of fit. *J Am Stat Assoc* 46(253):68–78
- Moukana JA, Koike K (2008) Geostatistical model for correlating declining groundwater levels with changes in land cover detected from analyses of satellite images. *Comput Geosci* 34(11):1527–1540
- Nelder JA, Mead R (1965) A simplex method for function minimization. *Comput J* 7(4):308–313
- Neshat A, Pradhan B, Javadi S (2015) Risk assessment of groundwater pollution using Monte Carlo approach in an agricultural region: an example from Kerman Plain, Iran. *Comput Environ Urban Syst* 50:66–73
- Neuman S, Jacobson E (1984) Analysis of nonintrinsic spatial variability by residual kriging with application to regional groundwater levels. *Math Geol* 16(5):499–521
- Nikroo L, Kompani-Zare M, Sepaskhah A, Fallah Shamsi S (2009) Groundwater depth and elevation interpolation by kriging methods in Mohr Basin of Fars province in Iran. *Environ Monit Assess* 166(1–4):387–407
- Olea RA (1999) *Geostatistics for engineers and earth scientists*. Kluwer Academic Publishers, New York
- Ouyang Y, Zhang JE, Ou LT (2006) Temporal and spatial distribution of sediment total organic carbon in an estuary river. *J Environ Qual* 35(1):93–100
- Papadopoulou MP, Varouchakis EA, Karatzas GP (2009) Simulation of complex aquifer behavior using numerical and geostatistical methodologies. *Desalination* 237(1–3):42–53
- Pardo-Iguzquiza E, Dowd P (2005) Empirical maximum likelihood Kriging: the general case. *Math Geol* 37(5):477–492
- Press WH, Teukolsky SA, Vetterling WT, Flannery BP (1992) *Numerical recipes in fortran*, 2nd edn. Cambridge University Press, New York
- Rivest M, Marcotte D, Pasquier P (2008) Hydraulic head field estimation using kriging with an external drift: a way to consider conceptual model information. *J Hydrol* 361(3–4):349–361
- Rivoirard J (2002) On the structural link between variables in Kriging with external drift. *Math Geol* 34(7):797–808

- Spiliopoulos I, Hristopulos DT, Petrakis E, Chorti A (2011) A Multigrid method for the estimation of geometric anisotropy in environmental data from sensor networks. *Comput Geosci* 37(3):320–330
- Sun Y, Kang S, Li F, Zhang L (2009) Comparison of interpolation methods for depth to groundwater and its temporal and spatial variations in the Minqin oasis of northwest China. *Environ Model Softw* 24(10):1163–1170
- Theodossiou N, Latinopoulos P (2006) Evaluation and optimisation of groundwater observation networks using the kriging methodology. *Environ Model Softw* 21(7):991–1000
- Tichy M (1993) *Applied methods of structural reliability*. Springer, Dordrecht
- Varouchakis EA (2012) Geostatistical analysis and space-time models of aquifer levels: application to mires hydrological basin in the prefecture of crete. PhD Thesis, Mineral Resources Engineering, Technical University of Crete, Chania
- Varouchakis EA (2016) Integrated water resources analysis at basin scale: a case study in Greece. *J Irrig Drain. E-ASCE* 142(3). doi:10.1061/(ASCE)IR.1943-4774.0000966
- Varouchakis EA, Hristopulos DT (2013a) Comparison of stochastic and deterministic methods for mapping groundwater level spatial variability in sparsely monitored basins. *Environ Monit Assess* 185(1): 1–19
- Varouchakis EA, Hristopulos DT (2013b) Improvement of groundwater level prediction in sparsely gauged basins using physical laws and local geographic features as auxiliary variables. *Adv Water Resour* 52(2013):34–49
- Varouchakis EA, Hristopulos DT, Karatzas GP (2012) Improving kriging of groundwater level data using nonlinear normalizing transformations—a field application. *Hydrol Sci J* 57(7):1404–1419
- Webster R, Oliver M (2001) *Geostatistics for environmental scientists: statistics in practice*. Wiley, Chichester
- Witten IH, Frank E, Hall MA (2011) *Data mining: practical machine learning tools and techniques: practical machine learning tools and techniques*. Elsevier, San Francisco
- Žukovič M, Hristopulos DT (2008) Environmental time series interpolation based on Spartan random processes. *Atmos Environ* 42(33): 7669–7678